*Desalination and Water Treatment*
www.deswater.com

doi:10.5004/dwt.2017.20658

76 (2017) 53–70
May

# Development of a flexible tool for the integrated techno-economic assessment of renewable desalination plants

Massimo Moser*, Franz Trieb, Jürgen Kern

*German Aerospace Center (DLR), Institute of Technical Thermodynamics, Wankelstrasse 5, 70563 Stuttgart, Germany, Tel. +49 711 6862-779, Fax +49 711 6862-8100, email: massimo.moser@dlr.de*

Received 7 May 2015; Accepted 28 February 2017

**ABSTRACT**

A number of simulation tools have been implemented in the past to assess the techno-economic feasibility of renewable power plants or desalination units. However, to the best of our knowledge, no well-established tool currently exists for the simulation of integrated renewable desalination plants on a system analysis level. This paper presents an innovative integrated methodology for the techno-economic assessment of renewable desalination plants. The technical assessment is performed within the simulation platform INSEL, whereas the existing model library – mainly consisting on photovoltaics (PV) and wind power – has been considerably extended by own developments. The newly implemented modules include a series of models for concentrating solar power (CSP) technologies such as Parabolic Trough, linear Fresnel and Central Receiver. In addition, models for thermal desalination such as MED and MED-TVC as well as for RO have been implemented. The technical model is typically used to perform annual yield analyses. The time step used for the input data such as meteorological data and demand data is of one hour. In a successive step the main results of the technical model are used as input for a flexible economic model, which has been developed as well within the context of this work. In the second part of the paper the developed methodology is applied within two exemplarily case studies in MarsaAlam, a touristic location in Egypt. In the first case study, several CSP technologies and configurations are compared. The second case study focuses on the optimization of the combined supply of desalinated water and electrical power.

*Keywords:* Integrated simulation tool; Renewable desalination; Techno-economic assessment; Solar energy; CSP; MED; SWRO

## 1. Introduction

Renewable technologies have achieved substantial capital cost reduction in the last years, driven by large scale market introduction. However, desalination powered by renewable energy is still not widely applied. Its development is limited to demonstration and small pilot plants which are mainly located in remote areas [1,2]. The feasibility of utility-scale renewable desalination plants still needs to be analyzed in detail by techno-economic models. The paper aims to the description of an innovative approach for the combined techno-economical assessment of renewable desalination on system analysis level. The paper is structured as follows: first, the state of the art of available tools for the simulation of renewable energy plants as well as desalination units is presented. Specific advantages and disadvantages of the respective tools are addressed. Second, the choice of the tool used for the analysis is justified, with particular focus to its advantages with respect to the objectives of this work. Third, the main features of each of the newly implemented modules, i.e. the CSP plant components as well as the desalination technologies are described. More detail about the models is given in the Appendix. Finally, the developed methodology for the integrated techno-economic assessment of renewable desalination plants

*Corresponding author.

*Presented at EuroMed 2015: Desalination for Clean Water and Energy Palermo, Italy, 10–14 May 2015. Organized by the European Desalination Society.*

is exposed. In addition, two case studies show exemplarily the capability of the developed tool.

## 2. Methodology for technical analysis

A number of simulation tools have been implemented to assess the techno-economic feasibility of renewable power plants or desalination units. However, to the best of our knowledge, no well-established tool currently exists for the simulation of integrated renewable desalination plants on a system analysis level. As an example, simplified tools (e.g. SAM [3], Greenius [4]) are well suited for quick generation of results, but are rather inflexible, i.e. the user has the possibility to select a limited number of configurations. On the other hand detailed thermodynamic programs exist (e.g. Ebsilon [5], Thermoflow [6]) which allow for flexible simulation of a large set of configurations, but are not adapted for the realization of an elevated number of parametric studies due to the high computational effort. In the Appendix (Table 9) a compact overview on key features of different simulation tools is presented [7–9]. Simulation of desalination processes typically has to be performed with separate tools such as DEEP [10], implemented by the International Atomic Energy Agency or specific programs such as ROSA [11], provided by the desalination company Dow Water.

In the light of the exposed considerations, an enhanced tool for the integrated analysis of renewable desalination should be a tool which combines the best features of the previously mentioned tools. After that a number of available programs have been screened, INSEL has been chosen as a well suitable option with regards to the objectives of this work [12]. INSEL is a simulation environment based on so-called "blocks". Blocks are symbols (i.e. graphical symbols within the user interface – Appendix, Fig. 13) which may represent any type of mathematical function, from a simple sum to a heliostat field model. Independently of the complexity of the mathematical formulation, each block is characterized by one or more "inputs" (i.e. independent variables), by a series of "block parameters" (i.e. constant values within a single simulation) and a number of "outputs" or results. The current version of INSEL includes PV modules, tracking systems, inverters, battery systems and wind turbines. In addition, the software allows for the creation of new, own-programmed models and their integration within the existing simulation environment. The technical assessment is then typically performed by means of annual yield analyses based on hourly simulation steps, i.e. within one simulation run each of the plant components is fed 8,760 times with the required input values such as meteorological input data as well as demand data. Within the context of this work, a number of new blocks for Concentrating Solar Power (CSP) and desalination processes have been developed. Such models include linear focusing CSP systems (Parabolic Trough (PT), linear Fresnel (LF)) and point focusing CSP systems (Central Receiver (CR)) as well as several heat transfer fluids (e.g. synthetic oil VP-1, molten salt (MS) and direct steam generation (Water/Steam)).The basics of the newly developed models are described in the following. More detail about the models is given in the Appendix, while the complete model setup can be found in [13].

### 2.1. CSP Model

#### 2.1.1. CSP solar field – parabolic trough (PT)

PT systems use parabolic mirrors to concentrate direct normal irradiance (DNI) onto a receiver located on the focal line of the parabola (Appendix, Fig. 14). Currently available collectors have an aperture width between 4.4 meters and 7.6 meters [14,15]. The typical optical concentration ratio is ca. 80. The main inputs, outputs and design parameters of the developed CSP PT model (or block) are listed in Table 1. The key input value is the DNI. Several loss mechanisms reduce the effectively available solar radiation onto the receiver. Some of these losses are due to non-ideal material properties and geometrical imperfections in the collector manufacturing [16]. Such impact is considered in the block parameter "collector type", which includes information about the collector geometry as well as the respective peak optical efficiency. Other losses are caused by the single-axis tracking and depend on the position of the sun and on the collector geometry [17–19]. The position of the sun is defined by the azimuth and the

Table 1
Summary of inputs, block parameters and outputs of the CSP solar field block

| Inputs |
|---|
| *Time (hour of the year), h* |
| *Azimuth angle,* ° |
| *Sun elevation angle,* ° |
| *DNI,* W/m² |
| *Ambient temperature,* °C |
| *Wind velocity,* m/s |
| *Storage state of charge,* $MWh_{th}$ |
| *Electricity demand,* $MW_{el}$ |
| **Block Parameters** |
| *Collector type*[1] |
| *Row distance,* m |
| *n subfields* |
| *HTF type*[2] |
| $T_{sf\_out\_design}$, °C |
| *Max. electricity demand,* $MW_{el}$ |
| *Solar multiple* |
| $\eta_{turb\_nom}$ |
| **Outputs** |
| $A_{sf}$,m² |
| *n collectors* |
| $\dot{Q}_{sf}$,$MW_{th}$ |
| $T_{sf\_out}$, °C |
| $\dot{Q}_{dump}$, $MW_{th}$ |
| $\dot{Q}_{startup}$, $MWh_{th}$ |
| $\eta_{sf}$ |
| $P_{parasitic\_sf}$,MWel |

[1]1 = LS-2; 2 = LS-3; 3 = SKAL-ET 150; 4 = SGX-1; 5 = AT150, [2]1 = oil (VP-1); 2 = solar salt; 3 = DSG (i.e. direct steam generation).

sun elevation angles, while the parameter "row distance" influences the shading losses.

The mentioned losses define the effective irradiance on the external surface of the receiver. After that, a share of the energy is transferred to the heat transfer fluid (HTF). The calculation of the solar field yield ($\dot{Q}_{sf}$) and of the solar field efficiency ($\eta_{sf}$) is based on the energy balance of the absorber tube, which includes a series of thermal losses as shown in Appendix, Fig. 15. The resulting energy balances and can be formulated according to [20] and [16] (Appendix, Eq. (3) and (4). Ambient temperature and wind velocity as well as the design outlet temperature from the solar collectors have an impact on the heat losses. The definition of the size of the solar field depends on the maximal electricity demand (i.e. nominal capacity of the steam turbine), on the nominal turbine efficiency and on the solar multiple. The solar multiple [Eq. (1)] is a non-dimensional parameter which is defined as the ratio between the heat collected by the solar field under design conditions and the nominal capacity of the turbine:

$$SM = \frac{\dot{Q}_{sf\_design}}{\dot{Q}_{turb\_in}} \quad (1)$$

This parameter is often used in order to simplify the comparison of different cases and configurations. On the basis of such information, the mirror area of the solar field ($A_{sf}$) as well as the number of collectors can be calculated. CSP PT plants typically present a layout with 4 subfields, whereas the power block is located at the center of the plant in order to minimize pressure and heat losses in the piping. Pumping requirements within the piping system are considerable and in oil-based systems may account to over 10% of the generated electricity under design conditions (depending on the SM). The calculation of the piping losses has been performed according to [21]. An important improvement of the developed CSP models in comparison to most existing steady-state models is the consideration of transient effects due to thermal inertia of different solar field components (HTF, receivers, piping system, etc.). These effects play an important role and their disregard leads to an overestimation of the solar field yield in the order of magnitude of 10–15% [22,23]. The impact of transients has been calculated with the lumped capacitance method described by [24] and [25]. Finally, the current state of charge of the thermal energy storage (TES) and the present electricity demand are required inputs of the PT model. Such two parameters are necessary to limit the solar field yield in some hours of the year. This may be the case when the TES is completely charged and the heat demand of the steam turbine is lower than the heat the solar field could potentially deliver. In such hours a share of the collected heat has to be dumped ($\dot{Q}_{dump}$).

#### 2.1.1.1. CSP solar field – central receiver (CR)

Central receiver systems consist of a large number of slightly curved mirrors called heliostats, which reflect direct solar radiation onto a receiver located at the top of a tower (Appendix, Fig. 14). The typical optical concentration factor ranges from 500 to 1,000 [26]. The implemented model uses a simplified procedure for the assessment of the heliostat efficiency, as presented in [27]. The heat transfer on the receiver of CR systems has been assessed according to [28,29] and can be formulated as in Eq. (5) (Appendix). The structure of the CR block with respect to the main inputs, outputs and block parameters is similar to that presented in Table 1 for the PT and therefore is not reported here.

#### 2.1.2. CSP thermal energy storage

The 2-tank molten salt storage concept is implemented in a large number of commercial parabolic trough CSP plants in Spain (e.g. Andasol). The typically used storage medium is a non-eutectic salt mixture consisting of 40 % potassium nitrate ($KNO_3$) and 60 % sodium nitrate ($NaNO_3$) [30]. The main inputs, outputs and design parameters of the developed TES block are reported in Table 2. The storage capacity is easily calculated as the ratio between the maximal electricity demand and of the design turbine efficiency – which gives the thermal input to the turbine under design conditions – multiplied by the equivalent full load storage hours ($FLH_{TES}$). Other design parameters are the temperatures of the cold and hot tanks, respectively, which are dependent on the limits imposed by the used salt mixture (min. design temperature of ca. 290°C, upper limit of 565°C due to corrosion problems at higher temperatures) as well as the HTF temperature at the outlet of the solar field [31].

Table 2
Summary of inputs, block parameters and outputs of the CSP thermal energy storage, [2]initial state of charge, [3]demand cover mode: 0 = demand cover with gross power; 1 = demand cover with net power

| Inputs |
|---|
| *Time (hour of the year)*, h |
| *Ambient temperature*, °C |
| $T_{HTF\_sf}$, °C |
| $\dot{Q}_{sf}$, $MW_{th}$ |
| *Electricity demand*, $MW_{el}$ |
| **Block parameters** |
| *Max. electricity demand*, $MW_{el}$ |
| $\eta_{turb\_nom}$ |
| $h_{TES\_design}$, h |
| $SoC_0$ [2] |
| $\dot{q}_{loss}$, %/d |
| $T_{hot\_tank}$, °C |
| $T_{cold\_tank}$, °C |
| **Outputs** |
| $Q_{TES\_design}$, $MWh_{th}$ |
| $Q_{TES}$, $MWh_{th}$ |
| *SoC* |
| $\dot{Q}_{turb}$, $MW_{th}$ |
| $T_{TES\_out}$, °C |
| $\dot{Q}_{cofir}$, $MW_{th}$ |
| $P_{parasitic\_TES}$, $MW_{el}$ |

Table 3
Overview of storage operation cases; $Q_{HX}$ = heat transferred to/from the TES through a heat exchanger; $t$ = time [13]

| Condition | Additional constraint | Storage operation |
|---|---|---|
| $Q_{sf} \geq Q_{turb\_target}$ | $Q_{TES(t-1)} + \lvert Q_{HX}\rvert \leq Q_{TES\_design}$ | Storage charge |
| | $Q_{TES(t-1)} + \lvert Q_{HX}\rvert > Q_{TES\_design}$ | Limited storage charge; → Partial solar field defocusing |
| $Q_{sf} \geq Q_{turb\_target}$ | $Q_{TES(t-1)} - \lvert Q_{HX}\rvert \geq 0$ | Storage discharge |
| | $Q_{TES(t-1)} - \lvert Q_{HX}\rvert < 0$ | Limited storage discharge; → Eventual fossil backup required |

In addition, the state of charge (*SoC*) at the beginning of the simulation and specific thermal loss coefficient ($\dot{q}_{loss}$) have to be defined.

According to the heat delivered by the solar field ($Q_{sf}$), the current SoC of the storage and the heat demand of the turbine $Q_{turb\_target}$, four TES operation cases (i.e. charging and discharging) are distinguished, as shown in Table 3. If the solar field delivers more energy than turbine and storage can accept, a share of the solar collectors is defocused, while in the case neither the solar field nor the TES are able to supply the required amount of heat to the turbine, a fossil backup would be necessary to completely satisfy the electricity demand.

The main outputs of the TES block are the design capacity of the thermal storage $Q_{TES\_Design}$, the current state of charge (*SoC*), the heat delivered to the turbine ($\dot{Q}_{turb}$) and the respective temperature $T_{TES\_out}$ as well as the parasitic power required to pump the HTF through the heat exchanger (in the case different fluids are used in the solar field and in the TES). Finally, during prolonged off-line periods may happen that the temperature on the cold tank falls below the design value. In this case additional fossil heat ($\dot{Q}_{cofir}$) has to be provided to avoid the freezing of the salt.

### 2.1.3. CSP power block (Rankine cycle)

The power block model consists of a conventional steam Rankine cycle, which can be fed by either solar or fossil-fuel-based heat. The implemented model bases on [32] and [33], typical values for CSP turbines derive from [34]. The key parameters (as shown in Table 4) are the heat flow at the inlet of the turbine ($\dot{Q}_{turb}$) and the steam conditions (temperature $T_{in}$ and pressure $p_{in}$). Also the number and the pressure level of the steam extractions for internal feed water pre-heating have been considered. Other important assumptions for the calculation of the electricity generation are the efficiency of the turbine stages, whereas a differentiation is made between high pressure and low pressure section, as well as the efficiencies of the feed water pump and of the generator. In addition four types of cooling can be selected, i.e. once-through, evaporative (or wet), dry cooling and MED. In the last case, the first chamber of the desalination plants acts as a condenser for the waste steam of the turbine. Relevant parameters for the cooling are ambient temperature (dry cooling), cooling water temperature (once-through cooling) as well as relative humidity and atmospheric pressure (evaporative cooling). Such cooling models bases on [19,32]. The details of the calculation procedure can be found in [13].

The model has also been adapted in order to take into account off-design conditions such as part load conditions and

Table 4
Summary of inputs, block parameters and outputs of the power block module

| Inputs |
|---|
| Time (hour of the year) |
| Electricity demand, $MW_{el}$ |
| $\dot{Q}_{turb}$, $MW_{th}$ |
| $T_{in}$, °C |
| $T_{amb}$ / $T_{cool\_water}$, °C |
| *Relative humidity* |
| $p_{atm}$, mbar |
| **Block parameters** |
| $P_{el\_nom}$, $MW_{el}$ |
| $T_{in\_design}$, °C |
| $p_{in\_design}$, bar |
| *Cooling type*[1] |
| *Co-firing switch*[2], y/n |
| *TTD*, K |
| *DCA*, K |
| $\eta_{gen\_design}$ |
| $\eta_{pump\_design}$ |
| $\eta_{exp\_design}$ |
| $T_{cool\_water\_design}$, °C |
| $T_{amb\_design}$[3], °C |
| *ITD*, K |
| $k_{startup}$ |
| **Outputs** |
| $P_{el\_gross}$, $MW_{el}$ |
| $\eta_{turb\_gross}$ |
| $\dot{Q}_{in}$, $MW_{th}$ |
| $\dot{Q}_{out}$, $MW_{th}$ |
| $\eta_{turb\_net}$ |
| *Part load* |
| $p_{cond}$, bar |
| $\dot{m}_{steam\_cond}$, kg/s |
| $T_{cond}$, °C |
| $P_{el\_net}$, $MW_{el}$ |
| $P_{el\_solar}$, $MW_{el}$ |
| $Q_{cofir}$, $MWh_{th}$ |
| $P_{parasitic\_pump}$, $MW_{el}$ |
| $P_{parasitic\_cool}$, $MW_{el}$ |
| $P_{parasitic\_plant}$, $MW_{el}$ |

[1]0 = once-through; 1 = MED; 2 = dry; 3 = evaporative tower; 4 = fixed pressure, [2]1 = ON; 0 = OFF, [3]relevant for cooling = 2–3; TTD = Terminal Temperature difference in HX; DCA = dry cooling approach in HX; ITD = initial temperature difference in dry cooling

start-up procedures. The calculation of the steam pressure in the different stages of the turbine under part load conditions is performed according to the Stodola´s theory [35], while the efficiencies of the turbine stages and the feed water pump efficiency are adjusted according to [36] and [37], respectively.

The main results of the power block model are gross and net electricity generation ($P_{el\_gross}$ and $P_{el\_net}$), net turbine efficiency ($\eta_{turb\_net}$), rejected heat flow ($\dot{Q}_{out}$) with its temperature ($T_{cond}$) and pressure ($p_{cond}$), solar share ($P_{el\_solar}$) as well as the own consumption for pumping ($P_{parasitic}$). Finally, Fig. 1 shows a screenshot of the INSEL user interface with the own-developed models for the simulation of a CSP central receiver plant. The time handling is performed by the time block (left side of Fig. 1). Next right to the time block, the sun calculation block assesses the exact position of the sun for each hour of the year, once the geographical coordinates (latitude, longitude) and the time zone of the analyzed location are known [17]. Hourly meteorological data such as direct normal irradiance (DNI), global horizontal irradiance (GHI), diffuse horizontal irradiance (DHI), ambient temperature and humidity, wind velocity as well as demand data (water demand, electricity demand) are read from an input file (grey block below the sun position block). The figure also shows the three main components of the CSP model, i.e. heliostat field and receiver, thermal energy storage (TES) and power block, respectively from the left to the right side of the screenshot.

## 3. Desalination models

### 3.1. Multi-effect distillation (MED)

The MED process consists of a series of evaporation chambers (Fig. 2). The feed water is sprayed by nozzles to the external surface of a tube bundle. The heat supply for the evaporation, which occurs on the tubes, is provided by condensation of steam flowing inside the tubes. The produced vapor acts in turn as a heat source in the successive stage. In the first effect, low pressure steam has to be externally supplied (e.g. waste heat from a steam turbine).

The MED model is based on [38] and [39]. This is in principle a 0-D model, meaning that each MED stage is described in the model as a point. Steady-state conditions, salt-free distillate as well as equal heat transfer area in all effects are assumed, the latter being a common practice in commercial desalination plants. The model consists of a set of equations and a number of empirical correlations for the

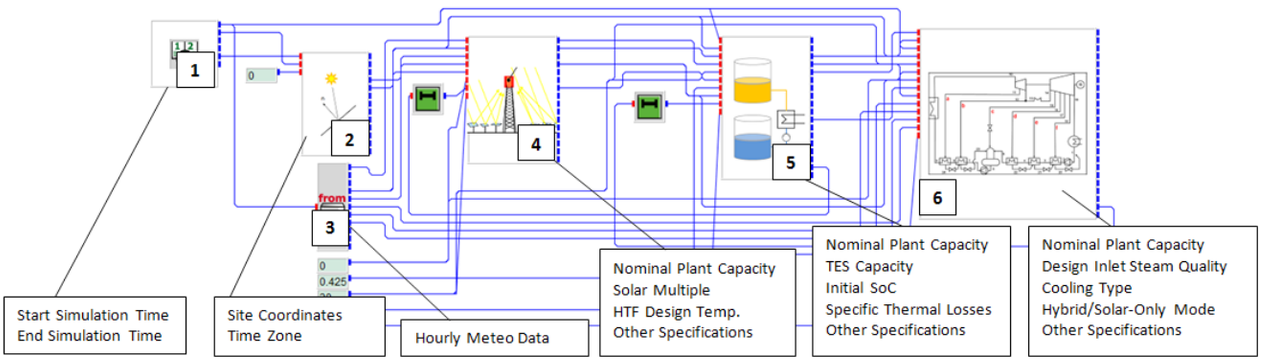


Fig. 1. Screenshot of the developed CSP INSEL models (central receiver) with specification of main design parameters (in the boxes) [13].

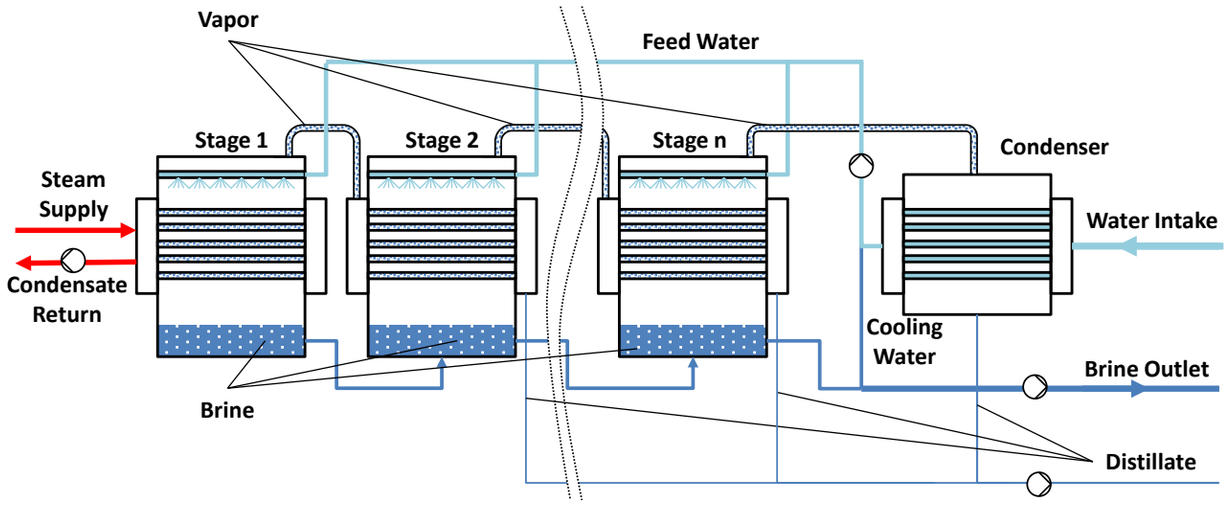


Fig. 2. Scheme of a MED process (parallel-cross configuration) – [13] Adapted from [38].

estimation of physical properties, thermodynamic losses and heat transfer coefficients. Due to the non-linearity of the correlations, an iterative solution procedure is required. Among different possible MED configurations, the parallel-cross feed layout has been selected for this work due to its high performance.

The main inputs, outputs and design parameters of the developed MED block are summarized in Table 5. The plant capacity is defined as a function of the available steam flow under design conditions ($\dot{m}_{steam\_cond}$), the number of stages and the resulting gain output ratio (GOR). The GOR in turn depends on the temperature conditions (steam supply temperature and cooling water temperature ($T_{seawater}$), the number of stages and the seawater salinity ($X_{seawater}$). A simplified intake model takes into account the power requirements for the cooling water and feed water supply.

Table 5
Summary of inputs, block parameters and outputs of the MED module

| Inputs |
|---|
| $\dot{m}_{steam\_cond}$, kg/s |
| $p_{steam\_cond}$, bar |
| $T_{seawater}$, °C |
| $X_{seawater}$, ppm |
| *Water demand*, m³/h |
| **Block parameters** |
| *TVC mode*[1] |
| *n stages* |
| $p_{motive\_steam\_design}$, bar |
| $\dot{m}_{motive\_steam\_design}$, kg/s |
| $T_{seawater\_design}$, °C |
| $X_{seawater\_design}$, ppm |
| $X_{max\_stages}$, ppm |
| $T_{steam\ (n=1)}$[2], °C |
| $\Delta t_{cond}$, K |
| *L intake pipe*, m |
| *intake pipe*, m |
| **Outputs** |
| *Plant capacity*, m³/d |
| $\dot{m}_d$, m³/h |
| *GOR* |
| $\dot{m}_{seawater}$, m³/h |
| $\dot{m}_{cool\_water}$, m³/h |
| $\dot{m}_{feed\_water}$, m³/h |
| $\dot{m}_{brine}$, m³/h |
| $\dot{m}_{discharge}$, m³/h |
| $T_{discharge}$, °C |
| $X_{discharge}$, ppm |
| *sA*, m²/(kg/s) |
| $sEC_{th}$, $kWh_{th}/m^3$ |
| $P_{parasitic\_MED}$, $MW_{el}$ |
| *sEC*, $kWh_{el}/m^3$ |

[1]0 = off; 1 = on, [2]relevant for TVC, [3]0 = off; 1 = on

The main results from the MED block are the drinking water production ($\dot{m}_d$), the seawater requirements ($\dot{m}_{seawater}$) as well as the characterization of the brine discharge flow (mass flow $\dot{m}_{discharge}$, temperature $T_{discharge}$ and $X_{discharge}$ salinity). Further relevant parameters with particular regard of the downstream economic evaluation are the specific surface of the heat exchangers (*sA*), the specific thermal consumption ($sEC_{th}$) and the electricity demand ($P_{parasitic\_MED}$).

Analogous to Fig. 1, Fig. 3 shows the minimal version of a MED model within the INSEL graphical user interface. The key design parameters for the simulation are also specified.

### 3.2. Reverse osmosis (RO)

Design and operation of RO plants is a function of a series parameters such as plant capacity, seawater quality (i.e. temperature, salinity and their seasonal variations) and required permeate composition (salinity, boron concentration etc.) [40]. The implemented model simulates a typical large-scale SWRO plant. The reference configuration is shown in Fig. 4. The pre-treated feed water enters the high pressure pump, where it reaches operating pressure. The required pressure has to overcome the sum of osmotic pressure at the end of the first stage and several other pressure losses such as frictional losses within the piping and in other equipment. After that, the pressurized water enters the first RO stage. Typically a RO stage consists of 6–8 membrane elements. Within the selected reference configuration, the permeate is separately collected at both ends of the stage, whereas the low-salinity permeate from the first three elements is blended with the permeate of the second stage, while the remaining permeate from the first stage passes through a booster pump and enters the second stage. The pressure applied by the booster pump is much lower than the pressure applied by the HP (high pressure) pump, due to the fact that in the salinity of the feed is much lower than in the first stage.

The RO model is based on [41] and [38]. The detailed calculation procedure can be found in [13]. Temperature and salinity of the feedwater as well as the water demand are required inputs for the model (Table 6). The key parameters of the RO model are the design product salinity ($X_{p\_design}$), the number of passes and their recovery rate (*RR* 1st Stage and *RR* 2nd Stage, respectively) as well as the number of elements per pass (n Elements 1st and n Elements 1nd, respectively) and the average age of the membranes, which impacts on both salt passage and permeability of the membranes. An overview of the design parameters of the used membranes for both the first and the second stage is reported in Appendix (Table 10). In addition, different intake types (e.g. open, submerged) and pre-treatment types (e.g. conventional, dissolved air flotation) can be selected.

The key results of the RO model are the permeate mass flow ($\dot{m}_p$) and its salinity ($X_p$), the feed operation pressure at the entrance of the first stage ($p_{feed\_1st\_stage}$), from which the electricity consumption (*EC*) can be calculated, the overall recovery ratio (*RR*) and the concentrate mass flow ($\dot{m}_{concentrate}$) as well as its salinity ($X_{concentrate}$). Finally, the total membrane area ($A_{membrane}$) represents one of the most important parameters for the economic evaluation. Fig. 5 shows the minimal version of a RO model within the INSEL graphical user interface. The key design parameters for the simulation are also specified.

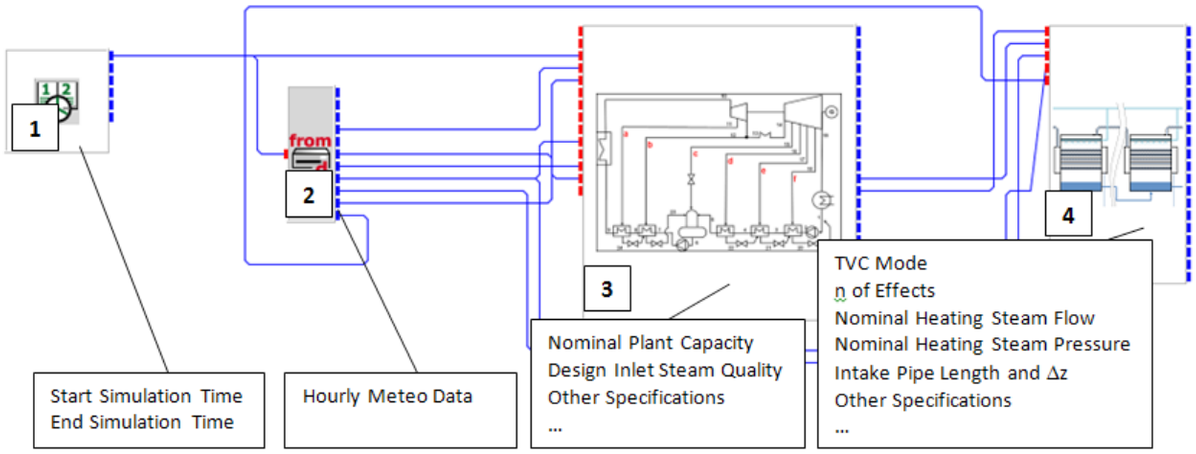


Fig. 3. Screenshot of the developed MED INSEL model with specification of main design parameters (in the boxes) [13].

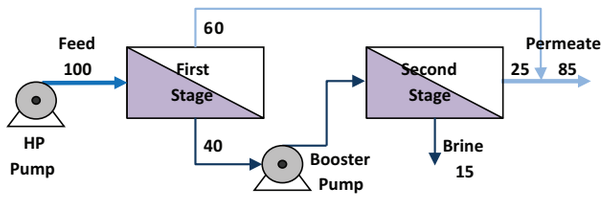


Fig. 4. Scheme of a SWRO plant with concentrate staging configuration – [13] Adapted from [41].

## 4. Methodology for economic analysis

The results of the technical model serve as input for the economic model. In this step, the capital expenditures (CAPEX) and the operational expenditures (OPEX) of each plant are assessed. The main outcomes of the economic model are the levelized electricity cost (LEC, [€c/kWh]) for each of the considered technologies and the levelized water cost (LWC, [€/m³]). In addition, the final comparison of combined power-and-water supply systems requires a common methodology which takes into account the specificities of the two considered systems. The approach proposed in this work is the calculation of the total cost of supply, which consists of the sum of the cost for electricity supply and for water supply [Eq. (2)]. In order to avoid the twofold consideration of the energy cost for desalination ($ENEX_{DES\ Plant}$), which appear both in the calculation of the power supply as well as in that of the desalination units), the cost of supply can be formulated as follows:

$$Supply\ Cost = \sum_{Power\ Plant=1}^{n} OPEX_{Power\ Plant} + \sum_{DES\ Plant=1}^{k} OPEX_{DES\ Plant} - ENEX_{DES\ Plant} \quad (2)$$

The CAPEX and OPEX assumptions base upon available literature and are summarized in the tables reported in Appendix (Table 11–15). The OPEX within Eq. (2) includes annual capital cost, personnel, equipment,

Table 6
Summary of inputs, block parameters and outputs of the block SWRO

| |
|---|
| Inputs |
| $T_{seawater}$, °C |
| $X_{seawater}$, ppm |
| *Water demand*, m³/h |
| Block parameters |
| $Water\ demand_{design}$, m³/h |
| $X_{p\_design}$, ppm |
| *RR 1st stage* |
| *RR 2nd stage* |
| *n elements 1st* |
| *n elements 2nd* |
| *Membrane age*, y |
| *Pre-treatment type*[1] |
| Δz *intake pipe*, m |
| *L intake pipe*, m |
| Outputs |
| $\dot{m}_{feed\_water}$, m³/h |
| $p_{(feed\_1st\_stage)}$, bar |
| $\dot{m}_{p}$, m³/h |
| $X_{p}$, ppm |
| *RR* |
| $\dot{m}_{concentrate}$, m³/h |
| $X_{concentrate}$, ppm |
| $A_{membrane}$, m² |
| *EC*, $MW_{el}$ |
| *sEC*, $kWh_{el}/m^3$ |
| $sEC_{intake}$, $kWh_{el}/m^3$ |

[1]pretreatment type: 1\ = conventional; 2\ = with DAF

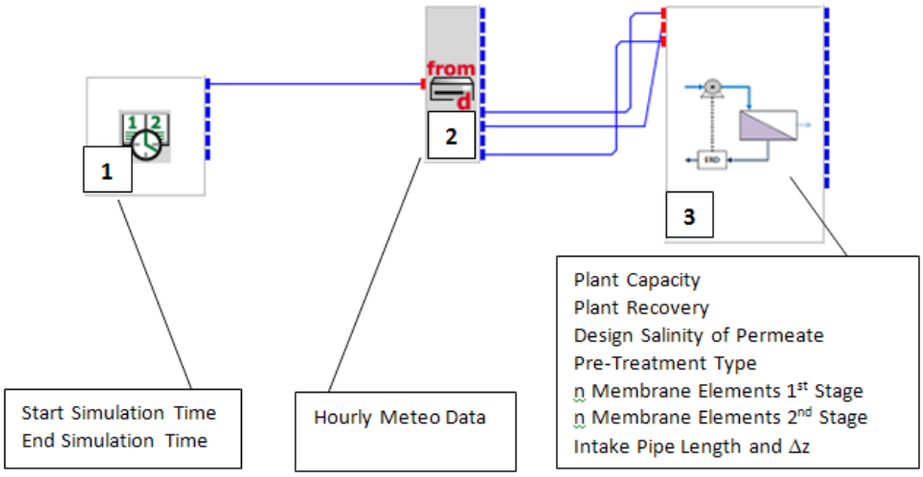


Fig. 5. Screenshot of the developed RO INSEL model with specification of main design parameters (in the boxes) – [13].

spare parts and insurance. The calculation procedure has already been presented in previous works [13,42] and therefore is not reported here. In addition, in order to cope with the large number of simulation runs, an automated tool for the generation and the evaluation of the economic results has been implemented (Appendix, Fig. 16).

## 5. Case studies

### *5.1. Overview*

This section exemplarily shows the potentiality of the developed methodology within two case studies:

- The first case study focuses on the technical and economic analysis of CSP technologies. The best performing CSP technology (i.e. collector type and heat transfer fluid) and configuration (i.e. solar field size and storage capacity) is then used as available option in the optimization procedure which is carried out within the second case study
- The second case study performs a comparison of optimized MED and RO systems taking into account the complete structure of the power supply. The available technologies for the power supply include renewable energy technologies such as CSP, PV and Wind Power as well as backup technology, whereas a conventional steam turbine has been assumed

The concluding section of this paper summarizes the main findings of the case studies pertaining to both technical and economic aspects and will indicate some suggestion for future research work.

### *5.2. Selected location and input data*

MarsaAlam (Egypt) has been selected as the location for the analysis. This city is not connected to the water, electricity and natural gas networks [43]. For this reason, this location is particularly attractive for the development of renewable desalination plants. The meteorological hourly data required for the INSEL simulations have been collected from [44–46]. The annual sum of direct normal irradiance (DNI) amounts to 2,530 kWh/m²/y, which is an excellent value if compared with other locations in the MENA region. The global horizontal irradiance (GHI) annual sum is slightly lower (2,386 kWh/m²/y). The DNI distribution over the selected year (Fig. 6) shows irradiation values higher than 200 kWh/m²/y in the period between May and November, while the minimum of DNI is in February with less than 140 kWh/m²/y.

The ambient temperature (monthly average) experiences a seasonal variation of around 10 K between approx. 20°C and 30°C, while the oscillation of the seawater temperature is of modest entity. Wind speed data originate from [46]. The annual wind speed average in MarsaAlam is approx. 7.0 m/s at 50 m height. The seawater salinity is slightly higher than 40,000 ppm and presents little seasonal variations. Fig. 7 shows the electricity demand in MarsaAlam: the averaged representation over the hours of the day and over the months of the year highlights that the electricity demand is mainly driven by cooling applications, as the demand is highest during the summer months and in particular during the early afternoon. The absolute values of the electricity demand ranges between 50 MW and 150 MW. The water demand to be covered by desalination is assumed to be constant at a value of 30,000 m³/d.

The assumed cost projections for renewable technologies in 2020 take into account cost reduction due to learning curves and economies of scale [47–50]. The cost of the fossil backup fuel refers to a crude oil price of $120/barrel in 2020 [51]. The optimization procedures performed in two proposed case studies base on these assumptions.

### *5.3. Case Study 1: Optimization of CSP plants*

The objective of the first case study is the optimization of a CSP plant. In other words, for a defined turbine capacity, the solar field size and the capacity of the ther-

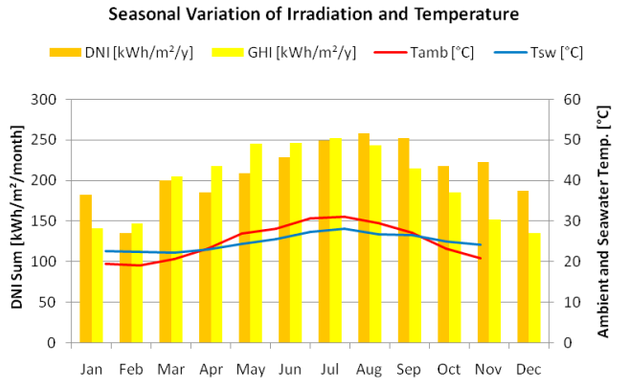


Fig. 6. DNI monthly sum, average ambient temperature ($T_{amb}$) and seawater temperature ($T_{sw}$) in MarsaAlam, Egypt [13].

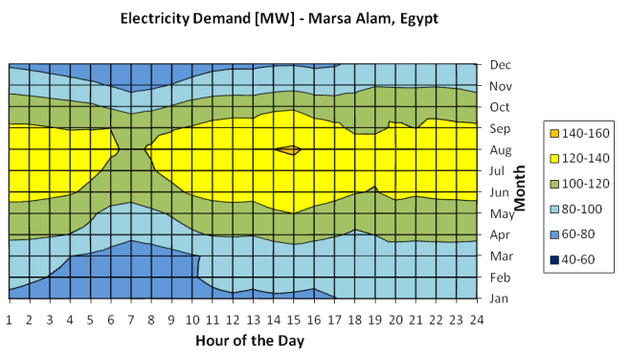


Fig. 7. Average electricity demand in MarsaAlam, Egypt [13].

mal energy storage have to be found which provides lowest LEC among all possible combinations. A series of annual yield calculations have been performed for a wide range of solar field sizes and thermal energy storage capacity. The LEC has been calculated for each of these configurations. The plant is assumed to operate in solar-only mode. This means that no fossil fuel is used for electricity generation. Only a small amount of fossil energy is required in order to eventually avoid the freezing of the storage material (freezing temperature approx. 240°C).

The results of the optimization procedure are summarized in Fig. 8. Such results refer to a Central Receiver CSP plant of the "Gemasolar" type. This plant uses a mixture of molten salts as the heat transfer fluid both for the receiver loop as well as for the storage loop. This particular layout allows for reaching high temperatures (approx. 565°C) and – accordingly – higher efficiencies than other CSP systems. A relatively broad LEC-minimum exists, which includes high SM (in the range 2.5–3.5) and high TES capacities (12–16 full load hours). A SM of 3.0 and a 14 FLH TES provides lowest LEC according to the economic assumptions.

The eventual choice of a non-optimal layout (e.g. TES over-sizing) would lead to high investment costs due to the installation of a large TES, which would be used inefficiently as it would often remain completely or partially discharged. On the contrary, an ideal utilization of the thermal energy storage would imply a daily complete charge–discharge cycle. Another non-optimal layout would imply the

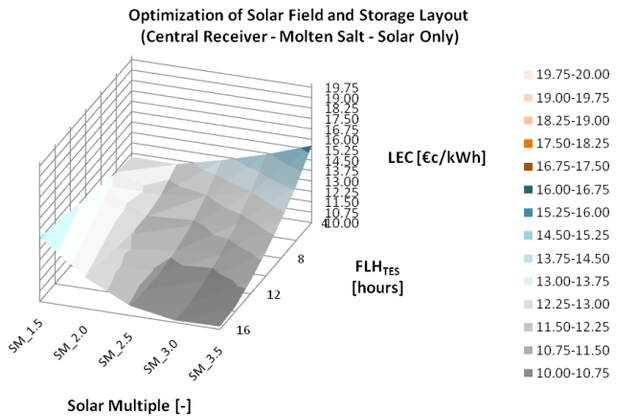


Fig. 8. Optimization of a molten-salt based Central Receiver CSP plant, MarsaAlam, Egypt, 2020 cost assumptions, solar-only operation [13].

oversizing of the solar field and the selection of a relatively small TES. In this last case, the storage would be mostly completely charged, while a relevant amount of heat from the solar field would have to be dumped. In both cases, the non-optimal layout of the plant components would lead to inefficiencies and – as a result – to higher LEC.

In order to find the most convenient CSP technology and configuration, the same optimization procedure as previously described has been applied to other CSP configurations. The analyzed cases include PT, LF and CR. In addition, three different heat transfer fluids have been selected, i.e. thermal oil (VP-1); molten salt (also: solar salt) and water/steam. This last layout also goes under the name of direct steam generation or DSG. In the case of the Central Receiver, only molten salt has been considered. This is due to the fact that the thermal oil suffers from an upper temperature limitation (393°C), while CR systems are best suited for the realization of temperatures higher than 500°C. Table 7 gives a summary of the specifications used for the INSEL simulations. According to the given specifications, highest gross turbine efficiency is reached in the case of the molten salt-based Central receiver (43.2%). For comparison, the efficiency of the VP-1 based Parabolic Trough is approx. 4.5 % lower.

The comparison of the three considered PT configurations shows that PT-SALT systems provide lowest LEC (Fig. 9). The main advantages are lower specific investment cost in comparison to PT-OIL plants. In fact, the molten salt-based CSP plants take advantage of an approx. 2.5 higher temperature difference between hot and cold tank in comparison to oil-based CSP systems. As a direct consequence, the required molten salt mass is significantly lower. Despite DSG systems are characterized by high efficiency and a simple plant layout, no proven TES concept for DSG is currently commercially available. This limits so far the economic attractiveness of such systems.

The LEC of PT, FR and CR ranges between 12.5 €c/kWh (PT) and 10.0 €c/kWh (CR). The main advantages of the Central Receiver technology are high geometrical efficiency along the whole year – which is mainly due to the 2-axis tracking of the heliostats –, high turbine efficiency as well as low heat requirements for anti-freezing purposes. FR plants

Table 7
CSP plant design data

| Solar field | Parabolic trough | Linear Fresnel | Central receiver |
|---|---|---|---|
| Collector type | SKAL-ET 150 | SUPERNOVA | Abengoa Heliostats |
| Collector aperture, m² | 817.5 | 741.9 | 121 |
| Collector spacing, m | 16.5 | 4.5 | Optimized by HFLCAL[2] |
| HTF | Oil/Solar salt/DSG | Oil/Solar salt/DSG | Solar Salt |
| Max HTF temperature[1], °C | 393/500/500 | 393/500/500 | 565 |
| Min HTF temperature, °C | 293 | | |
| Thermal energy storage | 2-tank molten salt storage (for VP-1 and solar salt); PCM for DSG | | |
| Cold tank temperature, °C | 285 (Anti-freezing if T < 270 °C) | | |
| Hot tank temperature, °C | 385–565 (dependent on HTF) | | |
| Power Block | Single-reheating | | |
| Cooling type | Evaporative cooling | | |
| Inlet steam pressure, bar | 100 | | |
| Inlet steam temperature, °C | 373–545 (dependent on HTF) | | |
| Gross turbine efficiency, % | 38.6[3]–42.6[4] | 38.6[3]–42.6[4] | 43.2[4] |

[1]values refer to different heat transfer fluids; [2]heliostat field layout calculation, tool developed by the Solar Research Institute of the DLR; [3]refers to synthetic oil (VP-1); [4]refers to molten salt, PCM = Phase change material, [13], based on [14,52–55].

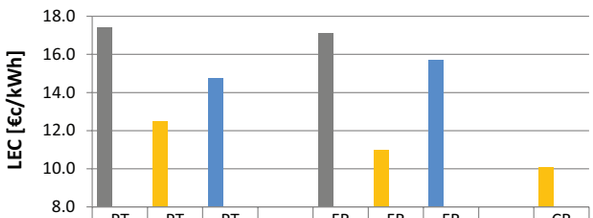


| | PT OIL | PT SALT | PT DSG | | FR OIL | FR SALT | FR DSG | | CR SALT |
|---|---|---|---|---|---|---|---|---|---|
| LEC | 17.40 | 12.48 | 14.76 | | 17.14 | 11.01 | 15.69 | | 10.08 |
| Solar Multiple | 3.00 | 3.00 | 1.25 | | 3.50 | 3.50 | 1.60 | | 3.00 |
| TES Capacity | 14 | 16 | 0 | | 14 | 14 | 0 | | 14 |

Fig. 9. Comparison of different CSP collectors and heat transfer fluids. The SM and the TES capacity of each of the shown configurations has been separately optimized; MarsaAlam, Egypt, 2020 cost assumptions, solar-only operation [13].

are characterized by simple layout, which allows avoiding additional components such as flexible joints and easy drainage. In addition, FR plants have high land use factor, i.e. the ratio between mirror area and required land area, which makes possible to minimize the land cost. However, FR systems are characterized by low geometrical efficiency and consequently lower heat collection in particular during off-design conditions.

### *5.4. Case Study 2: Optimized systems for the supply of water and electricity*

Aside from the optimization of single plants, e.g. renewable power plants as shown in the previous section as well as desalination plants [42], the developed methodologies and tools can be used for the assessment of combined supply systems. This is the main focus of the second case study. Within this analysis a comparison of optimized MED and RO systems is performed. Thereby the complete structure of the power supply is taken into account. The available technologies for the power supply include renewable energy technologies such as CSP, PV and Wind Power as well as a backup technology, whereas a conventional steam turbine has been assumed (Fig. 10). The analysis has been performed for a typical year with hourly resolution steps for meteorological and demand data. All analyzed configurations satisfy the same demand profiles for local power and water supply on an hourly basis, which allows for a fair comparison among competing scenarios.

Two main scenarios have been taken into account:

1. SWRO-Mix: in this case, the power fleet generates electricity in order to cover the total electricity demand, which consists of the sum of the demand for the local supply and of the demand for the SWRO plant. According to these requirements, the objective of the optimization procedure is the minimization of the LEC, without any further constrains.
2. MED-Mix: in comparison to the previous case, heat is required for the supply of the MED. The heat may be provided by the waste heat of a steam turbine (conventional or CSP). In this case, the minimization of the LEC cannot be used as the objective function, as heat cost would be neglected.

The assumed MED plant is a 13-stage unit with parallel-cross configuration. The pressure of the waste heat from the steam turbine is 0.35 bar. The resulting GOR is approx. 11.5. Concerning the SWRO, a partial two-pass configuration

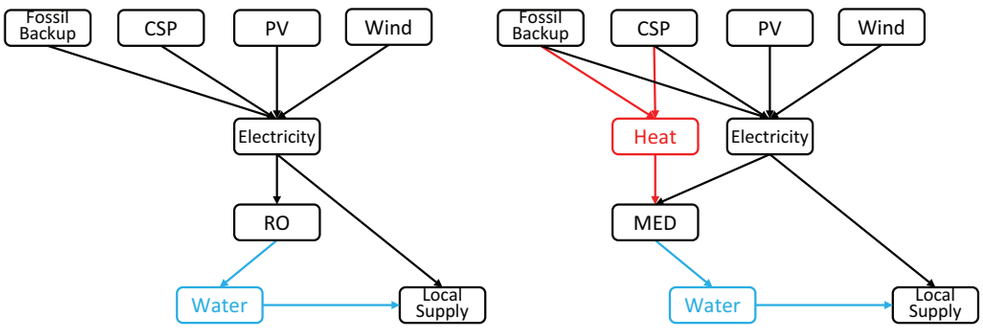


Fig. 10. The two considered options for the combined supply of water and electricity. Left: RO desalination; Right: MED desalination [13].

Table 8
Comparison of power plant configurations and key economic results of SWRO and MED power mix; Assumption: the power park is optimized for a fossil fuel price of 120 $/bbl

| Installed power capacity | Mix-SWRO | Mix-CSP-MED |
|---|---|---|
| CSP turbine capacity, MW | 50.0 | 50.0 |
| CSP solar multiple | 3.0 | 3.4 |
| CSP TES capacity, h | 14.0 | 15.0 |
| PV, MW | 70.0 | 45.0 |
| Wind, MW | 100.0 | 90.0 |
| Fossil backup, MW | 104.8 | 101.5 |
| Annual yield analysis | | |
| Renewable share, % | 76.6 | 73.8 |
| Electricity curtailment, %/annual demand | 1.7 | 7.1 |
| Annual demand, GWh/y | 899.3 | 873.2 |
| Specific cost of supply, €cent/kWh | 7.03[1]–9.62[2] | 6.89[1]–9.92[2] |
| LWC, €/m³ | 0.89[1]–0.98[2] | 0.99[1]–1.06[2] |
| Cost of supply, Mio. €/y | 69.7[1]–93.0[2] | 69.0[1]–95.8[2] |

[1]8 $/bbl; [2]120 $/bbl [13]

with conventional water pre-treatment has been assumed. The total recovery rate is approx. 42% and the product water salinity before post-treatment is approx. 100 ppm. The specific electricity consumption is 1.5 kWh/m³ and 4.2 kWh/m³ for MED and RO, respectively. An optimization has been carried out separately for the SWRO-Mix and for the MED-Mix scenarios, respectively. The main results are summarized in Table 8. The resulting power fleets include in both the SWRO case and the MED case all considered technologies. At a first sight, this may appear surprising, since each technology is characterized by specific power production patterns and by different cost. In particular, the cost optimal supply consists of both intermittent renewable energy sources (i.e. PV and Wind power) on the one hand, which provides relatively low LEC but cannot deliver power on-demand, and CSP as well as conventional backup on the other hand, which are slightly more expensive than PV and Wind power but are capable to provide high-quality dispatchable power. The dispatchability of CSP is guaranteed by the utilization of the thermal energy storage and -in the case the storage is completely discharged- by hybrid operation. In both the SWRO and the MED case, the optimal CSP capacity is 50 MW, which is slightly lower than the minimal annual power demand of 55 MW. The CSP plant is equipped with a large thermal energy storage (14–15 h) and the solar multiple is in both cases equal or higher than 3.0. Accordingly, the CSP plant is able to achieve approx. 7,500 FLH/y.

The installed PV and Wind power capacity are higher in the SWRO case (PV: 70 MW vs. 45 MW; Wind: 100 MW vs. 90 MW), which is mainly due to the different constrains in the two cases. In particular, in the SWRO case the CSP plant can act as a fully balancing renewable power plant. This behavior can be appreciated in Fig. 11, which shows the hourly electricity generation patterns for a typical winter week. Whenever the power production by intermittent renewables such as PV and Wind is high, the load of the CSP turbine can be reduced to a minimum. On the contrary, the CSP plant is operated at nominal conditions whenever the PV and Wind power is not sufficient to cover the demand. The fossil backup is used as "last-option" in order to cover the gaps in the power supply. In the SWRO case, the power curtailments (shaded areas above the demand line in Fig. 11) only amount to 1.7% of the total power demand on annual basis, while the renewable share (i.e. the annual renewable electricity generation divided by the total power demand) reaches 76.6%.

A comparison of Fig. 11 and Fig. 12 may help to highlight the main differences between SWRO-Mix and MED-Mix case. The two figures show the hourly power and water production patterns for a typical winter week in the SWRO-Mix and in the MED-case, respectively. The hourly dispatch model is quite straight-forward. Renewables are assumed to have feed-in priority as long as their power generation sum is lower than the load. This assumption is supported by the fact that renewable energy technologies – PV and wind power in particular – provide lower LEC than the backup power plant as long as world market fossil fuel prices are assumed. The backup power plants cover the remaining gaps at times of insufficient renewable electricity generation. If the sum of renewable electricity generation exceeds the load, two cases have to be differentiated. In the MED case, the CSP plant is operated at full load around-the-clock (Fig. 12) in order to guarantee continuous heat supply to the thermal desalination unit. In the RO case, CSP can be flexibly operated between full load and minimal load (Fig. 11). An empirical requirement has been introduced, which involves the minimum amount of secondary control reserve

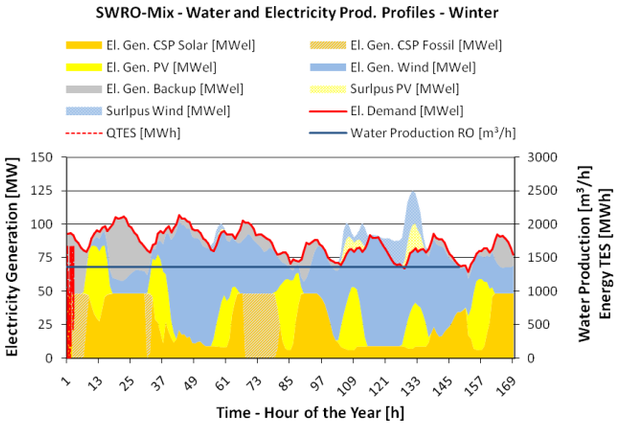


Fig. 11. Optimized SWRO-Mix- electricity and water production profiles in the first week of the year; 30,000 m³/d desalination capacity, MarsaAlam, Egypt, fossil fuel price 120 $/bbl, 2020 cost assumptions for renewable energies [13].

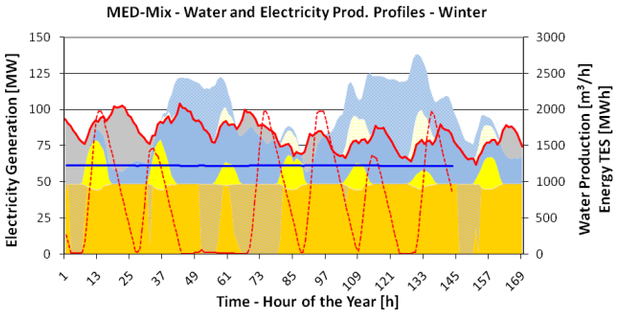


Fig. 12. Optimized MED-Mix- electricity and water production profiles in the first week of the year; 30,000 m³/d desalination capacity, MarsaAlam, Egypt, fossil fuel price 120 $/bbl, 2020 cost assumptions for renewable energies [13].

in order to avoid grid instability. This condition practically means that at least one turbine – i.e. either the backup power plant or the CSP turbine – has to be in operation at least at minimum load conditions (ca. 20% of the nominal load) in order to control sudden variations of electricity generation or of demand. Independently of the considered case, PV and wind power are curtailed if the sum of their electricity generation exceeds the residual load (i.e. the difference between actual load and CSP electricity generation).

In the MED case, due to the fact that the CSP turbine is forced to supply a constant heat load to the MED, the flexibility of the system is reduced. The intermittent electricity generation by PV and wind power can only be balanced by the conventional backup. Accordingly, optimal installed capacity of PV and Wind power is lower, while the curtailments are significantly higher than in the previous case (7.1 % of the total power demand on annual basis). In the end, such a difference is also responsible for the higher cost of supply in the MED-Mix case (95.8 [Mio. €/y] vs. 93.0 [Mio. €/y] in the SWRO case). The differences in the cost of supply also are reflected in the averaged electricity cost (SWRO: 9.62 [€c/kWh]; MED 9.92 [€c/kWh]) as well as in the levelized water cost (SWRO: 0.98 €/m³, MED: 1.06 €/m³).

## 6. Conclusions

This paper presents an innovative methodology for the integrated techno-economical assessment of utility-scale renewable desalination plants. Different types of renewable technologies (CSP, PV, Wind Power) as well as widely used desalination technologies like RO and MED have been considered within the models. The first part of the paper gives insight into the developed methodology for technical analysis. A brief introduction about the implemented economic model has been given as well, whereas a comprehensive overview can be found in previous publications of the author. In the following the potentiality of the implemented tool is exemplarily shown within two case studies. MarsaAlam in Egypt has been selected as the location for the analysis. In the first case study, the optimization of a CSP plant has been performed. Several CSP technologies such as linear focusing as well as point focusing collectors have been considered. The impact of key parameters such as solar field size and storage capacity on technical and economic performance has been evaluated. The economic analysis shows that for the selected site the molten salt based Central Receiver CSP presents the lowest levelized electricity cost. The advantages of the Central Receiver are the high conversion efficiency and the relatively low specific investment cost for the thermal energy storage, which leads to larger installed storage capacities and allows for the extension of plant operation also during evening and even night hours. The second case study aims at the identification of a cost optimal power plant fleet and desalination plant for the same site. The comparison of such systems relies on the average annual cost of supply. Two main scenarios, i.e. one SWRO case and a MED case have been considered and separately optimized. The results show that the cost optimal power fleet consists of a mix of intermittent renewable technologies such as PV and wind power as well as dispatchable technologies such as concentrating solar power (CSP) and conventional backup power plants. Concerning the comparison between RO and MED, RO provides approx. 10% lower levelized water cost than MED. The overall cost of supply are approx. 2.9% lower in the RO case, which is mainly due to the flexible CSP operation and to the consequently lower power curtailment. On the contrary, in the MED case the power supply system is less flexible, as the CSP is designated to continuously provide heat to the MED. Such a drawback may be reduced by the introduction of a low-temperature storage in order to decouple the supply of the MED from the operation of the turbine. Such an analysis will be performed in the framework of future research activities. In addition, future work may include the analysis of further sites, in particular at the countries of the Arabic Gulf, where the demanding feedwater pre-treatment in RO plants could still result in a preference for thermal desalination systems.

## Symbols

| | | |
|---|---|---|
| *A* | — | Area [m²] |
| *DHI* | — | Diffure horizontal irradiance [W/m²] |
| *DNI* | — | Direct normal irradiance [W/m²] |
| *EC* | — | Energy consumption [$MW_{el}$] |
| *ENEX* | — | Energetic expenditures [Mio. €/y] |
| *FLH* | — | Full load hour [h] |

*GHI* — Global horizontal irradiance [W/m²]
*GOR* — Gain output ratio [–]
*LEC* — Levelized electricity cost [€c/kWh]
*LWC* — Levelized water cost [€/m³]
$\dot{m}$ — Mass flow [kg/s]
*OPEX* — Operational expenditures [Mio. €/y]
*p* — Pressure [mbar]
*P* — Electrical powe [$MW_{el}$]
*Q* — Thermal energy [MWh]
$\dot{Q}$ — Thermal heat flow [$MW_{th}$]
*RR* — Recovery ratio [–]
*sA* — Specific heat transfer area [m²/(kg/s)]
*sEC* — Specific energy consumption [kWh/m³]
*SM* — Solar multiple [–]
*t* — Time [h]
*T* — Temperature [°C]
*X* — Salinity [ppm]
η — Efficiency [–]

## Abbreviations

CR — Central Receiver (Solar Tower)
CSP — Concentrating Solar Power
DCA — Drain Cooling Approach
DLR — German Aerospace Center
DSG — Direct Steam Generation
ITD — Initial Temperature Difference
LF — Linear Fresnel Reflector
HTF — Heat Transfer Fluid
HX — Heat Exchanger
INSEL — Integrated Simulation Environment Language
MED — Multi-Effect Distillation
MS — Molten Salt
PCM — Phase Change Material
PT — Parabolic Trough
PV — Photovoltaics
REMix-CEM — Renewable Energy Mix – Capacity Expansion Model
RO — Reverse Osmosis
SAM — System Advisor Model
SoC — State of Charge
TES — Thermal Energy Storage
TTD — Terminal Temperature difference
TVC — Thermal Vapor Compression

## Subscripts

*amb* — Ambient
*atm* — Atmospheric
*cond* — Condensation
*d* — Distillate
*el* — Electrical
*exp* — Expansion
*gen* — Generator
*nom* — Nominal
*p* — Permeate
*sf* — Solar Field
*sw* — Seawater
*th* — Thermal
*turb* — Turbine

## References


[1] A. Al-Kharagouli, L. Kazmerski, Energy consumption and water production cost of conventional and renewable-energy-powered desalination processes, Renew. Sustain. Energy Rev., 24 (2013) 343–356
[2] IRENA, ESTAP, Water Desalination Using Renewable Energy – Technology Brief, 2012.
[3] SAM, NREL, System Advisor Model, Online: https://sam.nrel.gov/ [Online: Apr. 2014].
[4] D.L.R. Greenius, H.T.W. Berlin, Greenius, Online: http://free-greenius.dlr.de/ [Online: Apr. 2014].
[5] EBSILON® Professional, STEAG Energy Services GmbH - System Technologies, Online: http://www.steag-systemtechnologies.com/ebsilon_professional+M52087573ab0.html [Online: Apr. 2014].
[6] Thermoflow Inc., Online: http://www.thermoflow.com/index.html [Online: Apr. 2014].
[7] L. Arribas, G. Bopp, M. Vetter, A. Lippkau, K. Mauch, Worldwide overview about design and simulation tools for hybrid PV systems, IEA 2011, Online [Nov. 2014]: http://www.iea-pvps.org/fileadmin/dam/public/ report/technical/rep11_01.pdf.
[8] Ho C., Software and Codes for Analysis of Concentrating Solar Power Technologies, SANDIA, 2008, SAND2008-8053.
[9] S. Mason, Worldwide overview of concentrating solar thermal simulation tools, paper presented at the SolarPACESConference 2011, Granada, Spain.
[10] DEEP – Desalination Economic Evaluation Program, International Atomic Energy Agency (IAEA), Online [Apr. 2014]: http://www.iaea.org/NuclearPower/Desalination/.
[11] ROSA – Reverse Osmosis System Analysis, Dow Water & Process Solutions, Online [Apr. 2014]: http://www.dowwaterandprocess.com/en/resources/rosa_system_design_software.
[12] INSEL, Integrated Simulation Environment Language, www.insel.eu.
[13] M. Moser, Combined Electricity and Water Production based on Solar Energy – Development of a flexible Simulation Tool for Modelling and Analysis of renewable Desalination, PhD thesis, Stuttgart University, 2015, http://dx.doi.org/10.18419/opus-2365.
[14] D. Kearney, Parabolic Trough Collector Overview, NREL Parabolic Trough Workshop, Golden CO, 2007
[15] K. Riffelmann, T. Richert, P. Nava, A. Schweitzer, Ultimate Trough ® – A significant step towards cost-competitive CSP, Energy Procedia., 49 (2014) 1831–1839.
[16] R. Forristall, Heat Transfer Analysis and Modelling of a Parabolic Trough Solar Receiver Implemented in Engineering Equation Solver, National Renewable Energy Laboratory Technical Report, NREL/TP-550-34169, 2003, Online [Nov. 2014]: www.nrel.gov/csp/troughnet/pdfs/34169.pdf.
[17] J.A. Duffie, W.A. Beckman, Solar Engineering of Thermal Processes, 1991, New York.
[18] V.E. Dudley, G.J. Kolb, A.R. Mahoney, T.R. Mancini, C.W. Matthews, M. Sloan, D. Kearney, Test Results - SEGS LS-2 Solar Collector. SANDIA Report, SAND94-1884, 1994.
[19] F. Trieb, S. Kronshage, V. Quaschning, J. Dersch, H. Lerchenmüller, G. Morin, A. Häberle, Solarthermische Kraftwerkstechnologie für den Schutz des Erdklimas - Technologiedatenbank und –modelle, 2004.
[20] J.F. Feldhoff, Vergleichende Analyse und Bewertung von Solarthermischen Kraftwerken mit solarer Direktverdampfung, Diploma Thesis, DLR and RWTH Aachen, 2007.
[21] M.J. Wagner, P. Gilman, Technical Manual for the SAM Physical Trough Model, NREL Report: NREL/TP-5500-51825, June 2011.
[22] T. Hirsch, H. Schenk, Dynamics of Oil-Based Parabolic Trough Plants – A detailed transient simulation model – Paper presented at the SolarPACES Conference 2010, Perpignan.
[23] J.F. Feldhoff, K. Schmitz, M. Eck, D. Laing, F. Ortiz-Vives, L. Schnatbaum-Lauman, J. Schulte-Fischedick, Comparative System Analysis of Parabolic Trough Power Plants with DSG and Oil using Integrated Thermal Energy Storage, paper presented at the SolarPACES Conference 2011, Perpignan.

[24] G. Mittelman, M. Epstein, A novel power block for CSP systems, Solar Energy, 84 (2010) 1761–1771.
[25] M. Cordes, Weiterentwicklung eines Solarfeldmodells für das Simulationstool INSEL mit anschließender Untersuchung regenerativer Energiesysteme, Diploma Thesis, University of Siegen, 2011.
[26] R. Buck, Solare Turmtechnologie - Stand und Potentiale, presentation at the solar colloquium 2008, Cologne, Germany.
[27] J. Dersch, P. Schwarzbözl, T. Richert, Annual yield analysis of solar tower power plants with GREENIUS, J. Solar Energy Eng., 133 (2011) 031017-031017-9.
[28] P. Schwarzbözl, M. Schmitz, R. Pitz-Paal, Visual HFLCAL – A software for layout and optimization of heliostat fields, paper presented at the SolarPACES Conference 2009.
[29] R. Pawellek, T. und Löw, T. und Hirsch, S. und Giuliano, P. und Schwarzbözl, Solar Tower Simulation with Ebsilon Professional. In: Proceedings of the SolarPACES 2011 conference. Sept. 2011, Spain.
[30] T. Bauer, D. Laing, R. Tamme, Recent Progress in Alkali Nitrate/Nitrite Developments for Solar Thermal Power Applications, Molten Salts Chemistry and Technology, MS9, Trondheim, Norway 5–9 June 2011.
[31] A. Gil, M. Medrano, I. Martorell, M. Lazaro, P. Dolado, B. Zalba, L.F. Cabeza, State of the art on high temperature thermal energy storage for power generation - Part 1: Concepts, materials and modellization.
[32] K. Strauß, Kraftwerkstechnik: zur Nutzung fossiler, nuklearer und regenerativer Energiequellen (VDI-Buch), Springer Verlag, 2007.
[33] K.H. Schüller, Repetitorium Wärmetechnik, Grundlagen, Auslegungen, Berechnungen, Energie & Management Verlagsgesellschaft, München, 1999.
[34] M.J. Montes, A. Abanades, J.M. Martinez-Val, M. Valdes, Solar multiple optimization for a solar-only thermal power plant, using oil as heat transfer fluid in the parabolic trough collectors, Solar Energy, 83 (2009) 2165–2176.
[35] H. Sigloch, Strömungsmaschinen – Grundlagen und Anwendungen – 2. Auflage, Hanser Verlag München Wien, 1993.
[36] A. Patnode, Simulation and Performance Evaluation of Parabolic Trough Solar Power Plants, Master Thesis University of Wisconsin- Madison, 2006.
[37] F. Lippke, Simulation of the Part Load Behavior of a 30MWe SEGS Plant, Prepared for Sandia National Laboratories, Albuquerque, NM, SAND95-1293, June 1995.
[38] J. Gebel, S. Yüce, An Engineer´s Guide to Desalination, VGB PowerTech, Essen, Germany, 2008.
[39] H.T. El-Dessouky, H.M. Ettouney, Fundamentals of Seawater Desalination, Elsevier, Kuwait University, 2002.
[40] H. Ludwig, SWRO Energy Consumption: Expectations and Reality for State-of-the-Art Technology, updated version of the paper presented at the IDA World Congress 2009, Nov. 7–9, Dubai.
[41] M. Wilf, L. Awerbuch, C. Bartels, M. Mickley, G. Pearce, N. Voutchkov, 2007, The Guidebook to Membrane Desalination Technology: Reverse Osmosis, Nanofiltration and Hybrid Systems Process, Design, Applications and Economics, L'Aquila.
[42] M. Moser, F. Trieb, T. Fichter, J. Kern, D. Hess, A flexible techno-economic model for the assessment of desalination plants driven by renewable energies, Desalination and Water Treatment, Desalination and Water Treatment 2014, DOI: 10.1080/19443994.2014.946718.
[43] M. Abou Rayan, B. Djebedjian, I. Khaled, S. El-Sarraf, Desalination option within water demand management and supply for Red Sea Coast in Egypt, paper presented at the 7th international Water Technology Conference, IWTC 2003, Cairo, Egypt.
[44] C. Hoyer-Klick, C. Schillings, SOLEMI - Solar Energy Mining, Online: www.solemi.de, DLR Institute of Technical Thermodynamics.
[45] Meteonorm Software: http://meteonorm.com.
[46] MERRA Database, Online [Nov. 2014]: http://gmao.gsfc.nasa.gov/research/merra, data analysis by DLR.
[47] C. Turchi, Parabolic Trough Reference Plant for Cost Modeling with the Solar Advisor Model (SAM), Technical NREL Report, NREL/TP-550-47605, July 2010.
[48] C. Turchi, G. Heath, Molten Salt Power Tower Cost Model for the System Advisor Model (SAM), Technical NREL Report, NREL/TP-5500-57625, February 2013.
[49] C. Singer, Doctoral Thesis: Solarturmreceiver für überkritische Dampfprozesse und ihre technische und ökonomische Bewertung, Springer Fachmedien, Wiesbaden 2013.
[50] Trieb, F., Schillings C., O´Sullivan M., Pregger, T., Hoyer-Click, C., Global Potential of Concentrating Solar Power, presented at the SolarPACES Conference 2009, Berlin, 2009
[51] F. Verdier, (Fichtner) F. Trieb, T. Fichter, M. Moser, (DLR) 2011. Desalination Using Renewable Energy, Task 2 - Energy Requirement, MENA Regional Water Outlook, Part II, Online [Nov. 2014]: www.dlr.de/tt/menawater.
[52] H. Price, E. Lüpfert, D. Kearney, E. Zarza, G. Cohen, R. Gee, R. Mahoney, Advances in parabolic trough solar power technology, J. Solar Energy Eng., 124 (2002) 109–125.
[53] NREL, System Advisor Model, Online [Apr. 2014]: https://sam.nrel.gov/.
[54] K.-J. Riffelmann, J. Kötter, P. Nava, F. Meuser, G. Weinrebe, W. Schiel, G. Kuhlmann, A. Wohlfahrt, A. Nady, R. Dracker, Heliotrough- A new collector generation for parabolic trough power plants, paper presented at the SolarPACES conference 2009, Berlin, Online [Nov. 2014]: http://www.heliotrough.com/doc/SolarPaces2009_Heliotrough.pdf.
[55] J. Kötter, K.J. Riffelmann, S. Decker, J. Fellmuth, A. Macke, P. Nava, G. Weinrebe, W. Schiel, A. Steindorf, R. Dracker, Helio trough: One Year Experience with the Loop in a Commercial Solar Power Plant, Proceedings of the 16th SolarPACES Conference, Perpignan, 2010.
[56] EnerMENA 2012 - H. Schenk, Yield Analysis for Parabolic Trough Solar Thermal Power Plants, Technical Report, 2012.
[57] CSP Today 2013 K. Chamberlain, CSP Parabolic Trough Report: Cost, Performance and Key Trends.
[58] G. Weinrebe, F. von Reeken, M. Wöhrbach, T. Plaz, V. Göcke, M. Balz, Towards Holistic Power Tower System Optimization, paper presented at the SolarPACES 2013, Las Vegas, Sept. 2013.
[59] A. Goodrich, T. James, M. Woodhouse, Residential, Commercial, and Utility-Scale Photovoltaic (PV) System Prices in the United States: Current Drivers and Cost-Reduction Opportunities, NREL Technical Report, NREL/TP-6A20-53347, February 2012.
[60] IRENA - working paper: Renewable Energy Technologies: Cost Analysis Series – Volume 1: Power Sector, Issue 4/5, Solar Photovoltaics, Jun. 2012.
[61] EPIA, main authors: G. Masson, M. Latour, M. Rekinger, I.-T. Theologitis, M. Papoutsi, Global Market Outlook for Photovoltaics 2013–2017.
[62] S. Tegen, E. Lantz, M. Hand, B. Maples, A. Smith, P. Schwabe, 2011 Cost of Wind Energy Review, NREL Technical Report, NREL/TP-5000-56266, March 2013.
[63] A.G. Prognos, F. Peter, L. Krampe, I. Ziegenhagen, Entwicklung von Stromproduktionskosten – Die Rolle von Freiflächen-Solarkraftwerken in der Energiewende, October 2013, Berlin.

## Appendix

Screening of available simulation tools for power supply and desalination plants

Table 9
Selection of available simulation tools [13], based on [7], [8], [9]; MSF = multi-stage flash; (y) = models under development

| Main application | System analysis simulation tools | | | | Thermodynamic cycle simulation tools | |
|---|---|---|---|---|---|---|
| Name | SAM | INSEL | TRNSYS | Greenius | EBSILON Professional | IPSEpro |
| Original purpose | System analysis of RE systems | System analysis of RE systems | Evaluation of solar systems for heating and cooling | System analysis of CSP systems | Engineering of conventional power cycles | Engineering of conventional power cycles |
| Developed by | NREL (based on TRNSYS) | doppelintegral | University of Wisconsin | DLR | Steag/DLR | SimTech simulation technology |
| Annual simulations (Time resolution) | y (hourly) | y (variable) | y (variable) | y (hourly) | y (mainly for design, hourly) | y (mainly for design, hourly) |
| User-required Know-how | Low/medium | Low/medium | Medium | Low | High | High |
| Simulation effort | Low | Low | Low | Low | Very high | Very high |
| User programming language | SamUL | FORTRAN, C, (MATLAB) | FORTRAN | Not implemented | EbsScript | Own developments possible |
| Models´ documentation | Partial | Partial | Open source | Medium | Good | |
| Available modules | | | | | | |
| PV | y | y (various types) | y | y | n | n |
| Wind | y | y (various types) | y | n | n | n |
| CSP | y (various types) | (y) (various types) | y | y | y (various types) | y (various types) |
| Other RE systems | Geothermal, biomass | Solar collectors, Buildings | Solar collectors, Buildings | n | n | n |
| Energy storage | Thermal | Thermal (molten salt, concrete), electrical | Thermal | Thermal | Thermal (molten salt) | Thermal (molten salt) |
| Desalination | n | (y) (MED/TVC /RO) | n | n | n | y - MED/TVC /RO/MSF |
| Economics | y | n | n | y | n | y |

### INSEL

INSEL is a short for Integrated Simulation Environment Language. The tool has been developed since more than 20 years at the Oldenburg University and at the Stuttgart University of Applied Sciences and is a commercially distributed product. INSEL is characterized by a comfortable graphical user-interface and by a modular structure, which allows for flexible and quick integration of new plant components. Sensitivity analyses and parametric studies can be alternatively carried out without the utilization of the graphical user-interface by means of batch scripts (e.g. ruby or python). Different languages such as FORTRAN, C/C++ and Matlab can be used for programming new modules. The procedure for the creation of new blocks is comfortable and user-friendly. Fig. 13 shows the screenshot of the INSEL user interface. The left bar includes the commercially available blocks (upper part) as well as the user blocks. The setup of a simulation in INSEL starts with the selection of a number of available blocks and their interconnection by mouse click. The user has to define the plant configuration to be analyzed. This could be for example a single CSP plant or a more complex mix of renewable energies, fossil backup and desalination. Fig. 13 also exemplarily includes the sequence of blocks which are used for the simulation of a Central Receiver (or Solar Tower) CSP plant in INSEL. Each of the main blocks has red input boxes on its left side, while

the blue boxes on the right side of the blocks are the outputs. The calculation typically takes 1–3 min, depending on the complexity of the model. The most important results can be extracted from the result tables and are graphically analyzed.

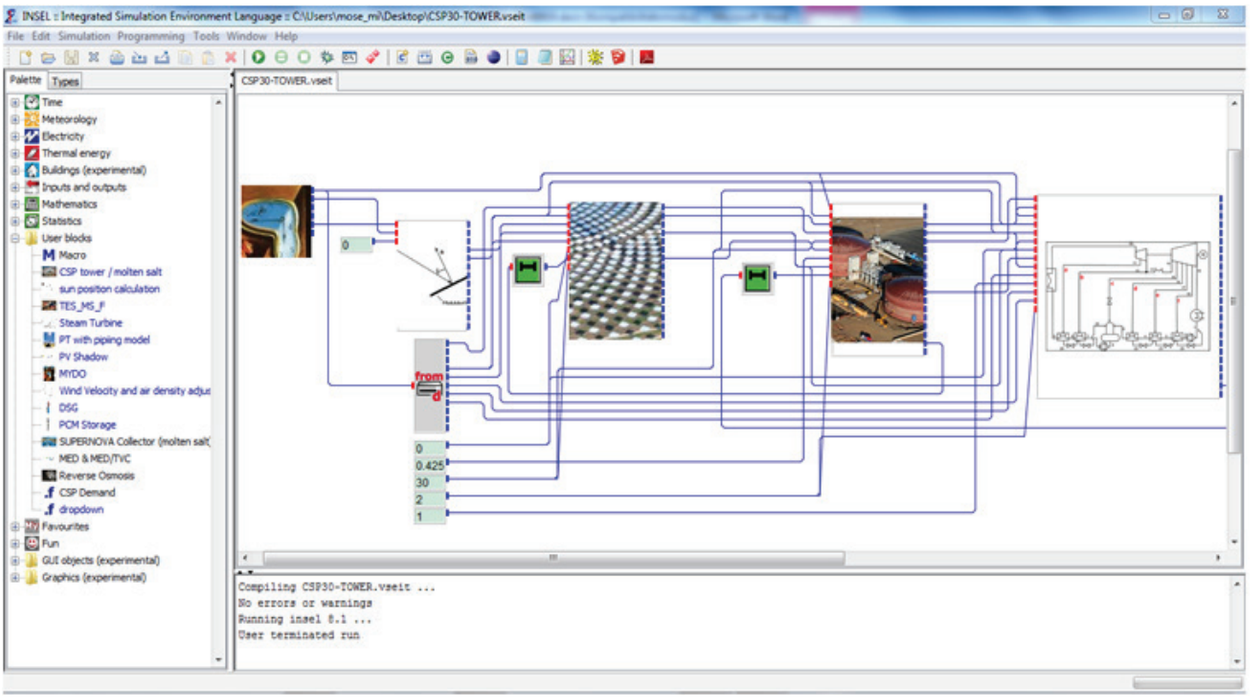


Fig. 13. Screenshot of the INSEL user interface with the simulation of a CSP Central Receiver plant [13].

INSEL is also linked with other tools used at DLR, e.g. REMix-CEM. This is a DLR in-house tool with focus on cost-optimal integration and commitment of renewable power plant portfolios in national or even international electricity supply systems. Within this tool, INSEL is used for the calculation of CSP, PV and Wind power plants' hourly power production profiles. Such profiles are then scaled during the REMix optimization process in order to find the lowest overall cost of supply.

**CSP solar field layouts**

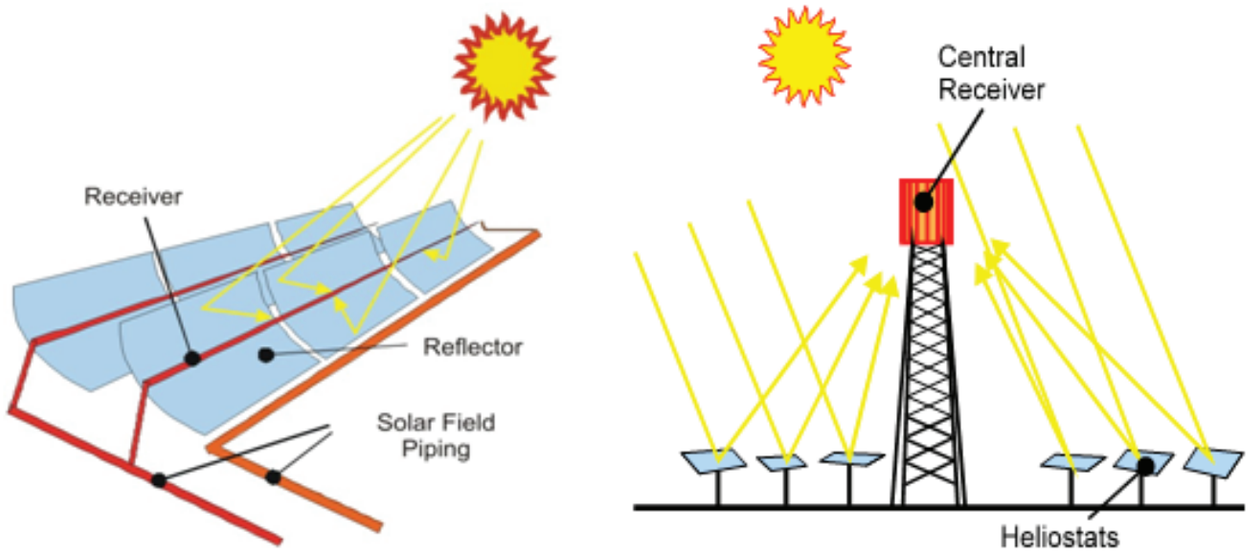


Fig. 14. Schematic view of a parabolic trough of a central receiver – Adapted from [56].

### CSP parabolic trough

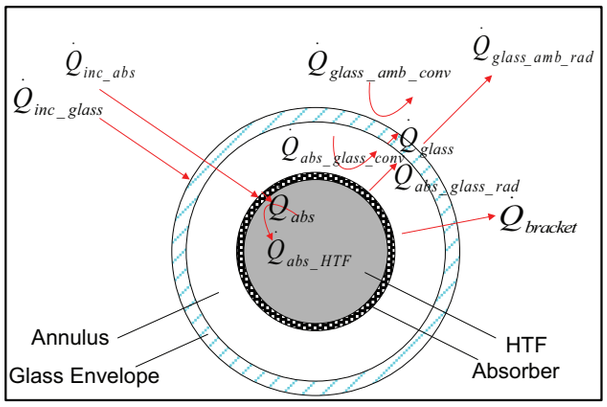


Fig. 15. Schematic of the radial heat flows between HTF, steel absorber, glass envelope and ambient [13], adapted from [16].

The energy balance can be formulated as follows. For the absorber:

$$\begin{cases} \dot{Q}_{inc\_abs} = \dot{Q}_{abs} + \dot{Q}_{abs\_glass} + \dot{Q}_{bracket} \\ \dot{Q}_{abs} = \dot{Q}_{abs\_HTF} \\ \dot{Q}_{abs\_glass} = \dot{Q}_{abs\_glass\_rad} + \dot{Q}_{abs\_glass\_conv} \end{cases} \quad (3)$$

The energy balance for the glass envelope leads to:

$$\begin{cases} \dot{Q}_{inc\_glass} + \dot{Q}_{abs\_glass} = \dot{Q}_{glass\_amb} \\ \dot{Q}_{abs\_glass} = \dot{Q}_{glass\_cond} \\ \dot{Q}_{glass\_amb} = \dot{Q}_{glass\_amb\_rad} + \dot{Q}_{glass\_amb\_conv} \end{cases} \quad (4)$$

CSP Heliostat Field and Receiver
The incident power $\dot{Q}_{inc}$ at the receiver is:

$$\dot{Q}_{inc} = DNI \cdot A_{sf} \cdot \rho_{refl} \cdot \eta_{sf} \cdot \eta_{wind} \cdot \eta_{focus} \quad (5)$$

| | | |
|---|---|---|
| $\dot{Q}_{inc}$ | [$MW_{th}$] | incident power |
| $\rho_{refl}$ | [-] | mirror average reflectivity |
| $\eta_{wind}$ | [-] | wind correction factor |
| $\eta_{focus}$ | [-] | focus factor |

### RO membranes design parameters

Table 10
Guideline for the selection of two-stages SWRO plants – [13], adapted from [40,41].

| Parameter | Unit | 1st Stage | 2nd Stage |
|---|---|---|---|
| Membrane type | – | SW5 or similar | ESPA4+ or similar |
| Recovery rate | % | 35–55 | 85–90 |
| Permeate flux | l/m²/h | 11–15 | 25–32 |
| Elements per vessel | – | 6–8 | 6–8 |
| Split partial ratio | % | 20–60 | – |

### Economic assumptions

Table 11
Overview and description of investment cost items of CSP CR plants with solar salt as HTF [13], based on [48,57,58] – I&C = instrumentation and control, *Ref. plant capacity: solar field 1,000,000 m², thermal energy storage 2,800 MWh, turbine 100 MW.

| CAPEX Item | Unit | Value |
|---|---|---|
| Land | €/m² | 1.8 |
| Site improvements | €/m² mirror | 15.7 |
| Solar field (excl. HTF) | €/m² | 132.4 |
| HTF system (incl. HTF) | €/m² | 0.0 |
| Tower | Mio. € | $=f(z_{tower}(Q_{rec}))$ |
| Receiver | €/$kW_{th}$ | 110.0 |
| Thermal storage | €/$kWh_{th}$ | 19.0 |
| BOS | €/$kW_{el}$ | 257.4 |
| Power block (Wet cooling) | €/$kW_{el}$ | 1007.8 |
| Power block (Dry cooling) | €/$kW_{el}$ | 1,183.8 |
| Fossil backup | €/$kW_{th}$ | 0.0 |
| Contingency | % of DC | 5.00% |
| EPC and owners´ cost | % of DC | 15.60% |
| OPEX item | | |
| Personnel cost | % DC/y | 0.40% |
| Equipment (spare parts) | % DC/y | 0.53% |
| Insurance rate | % DC/y | 0.50% |
| Misc. (utilities & contract services) | % DC/y | 0.30% |

Scale effects are taking into account according to [50].

Table 12
Overview of PV investment and operational costs [13], based on [51,59–61]; EPC = engineering, procurement and construction; *Ref. plant capacity 10 MWp, fix mounted

| CAPEX item | Unit | Value |
|---|---|---|
| Land | €/m² | 1.8 |
| Site improvements | €/m² module | 11.7 |
| Modules | €/$kW_p$ | 947.7 |
| Inverters | €/$kW_p$ | 155.5 |
| Electrical works | €/$kW_p$ | 190.0 |
| Mounting structure | €/$kW_p$ | 224.5 |
| Tracking system | €/$kW_p$ | 0.0 |
| Civil works | €/$kW_p$ | 165.1 |
| Contingency | % of DC | 1.00% |
| EPC and owners´ cost | % of DC | 8.00% |
| OPEX item | | |
| Personnel | % DC/y | 0.63% |
| Water | % DC/y | 0.06% |
| Spare parts | % DC/y | 1.00% |
| Insurance | % DC/y | 0.50% |

Table 13
Overview and description of investment cost items of wind power plants [13], based on [51,62,63]; EPC = engineering, procurement and construction, *Ref. plant capacity 10 MW

| CAPEX item | Unit | Value |
|---|---|---|
| Wind turbine | €/kW | 1,034.4 |
| Grid connection | €/kW | 134.9 |
| Construction | €/kW | 135.6 |
| Other capital cost | €/kW | 52.2 |
| Contingency | % of DC | 5.55% |
| EPC and owners´ cost | % of DC | 1.44% |
| OPEX item | | |
| Personnel | % of DC | 0.53% |
| Spare parts | % of DC | 1.50% |
| Insurance | % of DC | 0.75% |

Table 14
MED plant capital cost; assumption: 14-stage evaporator, 100,000 m³/d capacity [13], based on [51]; I&C = instrumentation and controls

| CAPEX item | Unit | Value |
|---|---|---|
| Intake , pump station and outfall incl. civil | $/(m³/d) | 500 |
| Seawater chlorination | $/(m³/d) | 20 |
| Process incl. Electrical and I&C | $/(m³/d) | 1,810 |
| Steam supply and condensate return | $/(m³/d) | 72 |
| Erection, commissioning and testing | $/(m³/d) | 181 |
| Potabilization plant | $/(m³/d) | 100 |
| Drinking water storage & pumping | $/(m³/d) | 100 |
| Auxiliary systems | $/(m³/d) | 50 |
| Civil works MED | $/(m³/d) | 91 |
| Civil infrastructure | $/(m³/d) | 30 |
| Electrical works excluding MED | $/(m³/d) | 30 |
| I&C works excluding MED | $/(m³/d) | 15 |
| Direct cost | $/(m³/d) | 2,999 |
| Contingencies | % of direct cost | 5.0 |
| Total MED plant | $/(m³/d) | 3,149 |

A detailed MED OPEX breakdown can be found in [13]. Scale effects are taken into account according to [38].

Table 15
SWRO plant capital cost; assumption: two-pass system, conventional pre-treatment, 100,000 m³/d capacity [13], based on [51]

| CAPEX item | Unit | Value |
|---|---|---|
| Intake , pump station and outfall | $/(m³/d) | 300 |
| Pretreatment system | $/(m³/d) | 250 |
| Membranes (without vessels) | $/(m³/d) | 80 |
| Reverse osmosis without membranes | $/(m³/d) | 720 |
| Potabilization plant | $/(m³/d) | 100 |
| Drinking water storage & pumping | $/(m³/d) | 100 |
| Wastewater collection & treatment | $/(m³/d) | 50 |
| Auxiliary systems | $/(m³/d) | 70 |
| Civil works | $/(m³/d) | 160 |
| Electrical works | $/(m³/d) | 150 |
| I&C works | $/(m³/d) | 70 |
| Total | $/(m³/d) | 2,050 |
| Contingencies | % DC | 103 |
| Total SWRO Plant | $/(m³/d) | 2,153 |

A detailed MED OPEX breakdown can be found in [13]. Scale effects are taken into account according to [38].

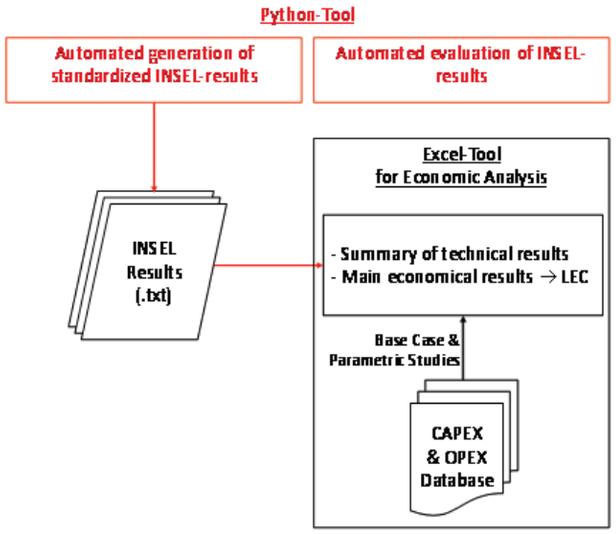


Fig. 16. Structure of the python tool for the automated generation and economic evaluation of INSEL results.